

## The Use of the BE SBS Algorithm to Evaluate Boundary and Interface Stresses in 3D Solids

F.C. de Araújo<sup>1,2</sup>, C. R. da Silva Jr.<sup>1</sup> and M. J. Hillesheim<sup>1</sup>

**Abstract:** In this paper, the BE SBS (subregion-by-subregion) algorithm, a generic substructuring technique for the BEM, is applied to evaluate stresses at boundary and interfacial points of general 3D composites and solids. At inner points, regular boundary integration schemes may be employed. For boundary or interfacial points, the Hooke's law along with global-to-local axis-rotation transformations is directly applied. In fact, in thin-walled domain parts, only boundary stresses are needed. As the SBS algorithm allows the consideration of a generic number of subregions, the technique applies to the stress analysis in any composite and solid, including the microstructural (grain-by-grain) modeling of materials. The independent assembly and algebraic manipulation of the BE matrices for the many substructures involved in the model, makes the formulation very suitable for dealing with large-order models, as it typically happens in the 3D microstructural analysis of general composites. For that, Krylov solvers were incorporated into the SBS algorithm. To show the performance of the technique, stresses are calculated in beams, and 3D representative volume elements (RVEs) of carbon-nanotube (CNT).

**Keywords:** 3D boundary-element models, subregion-by-subregion algorithm, general composites, stress analysis, Krylov solvers.

### 1 Introduction

In Araújo and Gray (2008), and Araújo, d'Azevedo, and Gray (2011), all the formulation details involved in the development of the subregion-by-subregion (SBS) algorithm considered for the analyses in this paper are shown. This algorithm is essentially a Domain Decomposition Method (DDM), wherein the definition domain of a certain problem is subdivided into a given number of subdomains or substructures, which are independently modeled and solved along with the available coupling conditions by means of the use of iterative solvers. Notice that subre-

---

<sup>1</sup> Dept. of Civil Eng., UFOP, Ouro Preto, MG, Brazil.

<sup>2</sup> Corresponding author. Email: dearaujofc@gmail.com

gioning strategies are fundamental for the BEM either for solving heterogeneous problems or developing parallel-computing codes or for combining the BEM with other methods, e.g. for developing BE-FE hybrid formulations [Araújo (1994); Araújo, d'Azevedo, and Gray (2010)]. The SBS strategy may be especially relevant for the grain-by-grain modeling of polycrystalline materials [Benedetti and Aliabadi (2013)], and for analyzing engineering systems involving nanomaterials as CNT-reinforced polymers [Srivastava and Atluri (2002)]. In fact, as in the case of nanosystems, more adequate molecular-dynamics-based (MD) formulations [Ghoniem and Cho (2002)] are, even for present-day computers, very time-consuming or prohibitive [Namila, Chandra, Srinivasan, and Chandra (2007)], continuum-mechanics-based (CM) formulations have been successfully considered instead (Kitipornchai, He, and Liew 200; Pantano, Parks, and Boyce 200; Wang, Ma, Zhang, and Ang 2006, and the BE-SBS strategy may be a very promising technique to deal with this kind of analysis [Araújo and Gray (2008); Araújo, d'Azevedo, and Gray (2011)].

In the particular case of the SBS algorithm, a very interesting point is the use of Krylov solvers, which, besides allowing the independent treatment of the substructures involved in the problem, also embeds a spontaneous parallelism to the technique. In fact, these characteristics of the SBS algorithm make it very convenient for dealing with very large models, including those resulting from the microstructural analysis of composites and other materials [Benedetti and Aliabadi (2013); Dong and Atluri (2012); Dong and Atluri (2013)]. In general, direct solvers present the following disadvantages: they may be exceedingly CPU time-consuming and memory-consuming for large-order models, and their parallel implementation is awkward. However, devising reliable efficient iterative solvers for non-symmetric systems of equations, as BEM systems typically are, has been a truly tough problem, and, despite the number of outstanding up-to-date works in this area, iterative solvers for general non-symmetric matrices are a still open question concerning convergence reliability [Barrett et al., (1996)]. In general, Krylov solvers [van der Vorst (2003)] are virtually the only possible alternatives for dealing with non-Hermitian systems, and among them, the short-recurrence ones (Bi-CG and variants) remain the most attractive options as much less memory compared to long-recurrence algorithms (GMRES and variants) is required.

Concerning the Bi-CG method, the most serious problem associated with it is its erratic convergence behavior, sometimes leading to non-convergence of the iterative solution process. To fix this disadvantage of the method, modified hybrid solvers have been derived by combining the Bi-CG solver with residual-minimization methods, as the GMRES. Thus, solvers as the Bi-CGSTAB( $l$ ) [Sleijpen and Fokkema (1993)], and the generalized product Bi-CG [GPBi-CG, Zhang (2002)] have been

devised. Additionally, preconditioners may be employed to accelerate the iterative process (van der Vorst 2003; Chen 2005). In recent works, the SBS technique itself has been used to construct efficient general preconditioners for BEM systems [Araújo, d’Azevedo, and Gray (2011)]. In the applications here, not especially focused on the performance assessment of the iterative solver, the BiCG solver with or without the SBS-based preconditioning is applied.

In this paper, techniques for calculating the stresses in solids and general composites are incorporated into the SBS-based computational code. For non-thin-walled solids or for internal points relatively far to the boundary, regular techniques based on boundary-integral stress representations with the use of special integration techniques are considered. For boundary nodes and for thin-walled solids, a special technique based on the direct application of the Hooke’s law is implemented. In this technique, the strain and corresponding stress tensors are calculated with respect to a local coordinate system wherein one of the axes is the outward normal vector to the boundary. All the necessary expressions for calculating these quantities are shown in the paper. Beams and representative volume elements (RVEs) of carbon-nanotube (CNT) composites are simulated to show the relevance of the technique for calculating stresses.

## 2 The preconditioned BE-SBS algorithm

In fact, the boundary-element substructuring-by-substructuring (BE-SBS) algorithm consists of a totally generic technique to decompose a problem domain into any number of subdomains or substructures. Roughly speaking, this technique is comparable to the element-by-element (EBE) technique, developed to finite-element (FE) analyses [Hughes, Levit, Winget (1983)], wherein a subdomain corresponds to a finite element. Thus, if needed, we can have a subregion mesh as fine as a FE mesh, and if the BE global system matrix were explicitly assembled, it would be highly sparse as well. As explained in previous papers [Araújo and Gray (2008); Araújo, d’Azevedo, and Gray (2011)], the BE-SBS algorithm embeds Krylov iterative solvers, and the global response for a problem is obtained by working exclusively with its local full-populated subsystems of equations with no global explicit assembly of system matrix; no zero blocks are stored or handled at all. The boundary conditions are introduced during the matrix assembly for each subsystem, and the interface conditions (between the subdomains), given by

$$\begin{cases} \mathbf{u}_{ij} = \mathbf{u}_{ji} \\ \mathbf{p}_{ij} = -\mathbf{p}_{ji} \end{cases} \quad \text{at } \Gamma_{ij} \quad (1)$$

are directly (not iteratively) imposed in the matrix-vector products during the iterative solution process. For  $n_s$  subregions, after introducing the boundary conditions,

the BE global system of equations is then given by

$$\sum_{m=1}^{i-1} (\mathbf{H}_{im}\mathbf{u}_{mi} - \mathbf{G}_{im}\mathbf{p}_{im}) + \mathbf{A}_{ii}\mathbf{x}_i + \sum_{m=i+1}^{n_s} (\mathbf{H}_{im}\mathbf{u}_{im} + \mathbf{G}_{im}\mathbf{p}_{mi}) = \mathbf{B}_{ii}\mathbf{y}_i, \quad i = 1, n_s, \quad (2)$$

where  $\mathbf{H}_{ij}$  and  $\mathbf{G}_{ij}$  denote the regular BE matrices obtained for source points pertaining to subregion  $\Omega_i$  and associated respectively with the boundary vectors  $\mathbf{u}_{ij}$  and  $\mathbf{p}_{ij}$  at  $\Gamma_{ij}$ . Note that if  $i \neq j$ ,  $\Gamma_{ij}$  denotes the interface between  $\Omega_i$  and  $\Omega_j$ ;  $\Gamma_{ii}$  is the outer boundary of  $\Omega_i$ . The  $n_s$  systems in (2) are the independent systems associated with each subregion of the problem, and which are separately considered in the calculations of the matrix-vector products needed for the iterative solver.

Additionally, to accelerate the iterative solver, a global SBS-based block-diagonal preconditioner, constructed by taking the diagonal blocks of the coupled system is considered,  $\mathbf{Q}_i$ , which for a generic number of subregions are given by

$$\mathbf{Q}_i = \begin{bmatrix} -\mathbf{G}_{i1} & \cdots & -\mathbf{G}_{i,i-1} & \mathbf{A}_{ii} & \mathbf{H}_{i,i+1} & \cdots & \mathbf{H}_{in} \end{bmatrix}, \quad i = 1, n_s \quad (3)$$

where the  $\mathbf{Q}_i$  matrices are straightforwardly formed from the subregion matrices of the model at hand. To store this preconditioner, an additional memory space of the size  $(nno \times ndofn) \times (nno \times ndofn)$  should be allocated, where 'nno' is the number of nodes of the model, and 'ndofn' is the number of degrees of freedom per node.

### 3 The calculation of stresses

Considering the  $O(r^{-3})$  and  $O(r^{-2})$  singularities of the fundamental kernels involved in the boundary integral expressions for evaluating the strain and stress tensors at a given point of a solid, the calculation of these quantities is a tough problem to deal with as special integration algorithms for dealing with the singularities at hand have to be devised. This is particularly difficult in case of the calculation of stresses at boundary nodes or in case of general thin-walled solids, wherein all the points of the solid are either at the boundary or very close to it (Fig. 1). To avoid directly facing the singular integrals appearing in the stress integration kernels, the stress tensor at boundary nodes can be directly determined from the boundary displacement field by means of the Hooke's law referred to a local system (Brebbia, Telles, and Wrobel 1984). In the procedure presented in Brebbia, Telles, and Wrobel (1984), one takes a local, mutually orthogonal  $\bar{x}_1$ - $\bar{x}_2$ - $\bar{x}_3$  coordinate system centered at the point where the boundary stresses should be calculated, and wherein the  $\bar{x}_3$  axis is defined by the outward normal vector, and the  $\bar{x}_1$  and  $\bar{x}_2$  axes by two tangential vectors at the boundary point (Fig. 2). In the code, stresses are particularly calculated at the element nodes. After the boundary solution has been completely

determined, the stress components referred to the local system shown in Fig. 2 are then given by:

$$\begin{aligned}
 \bar{\sigma}_{13} &= \bar{\sigma}_{31} = \bar{p}_1 \\
 \bar{\sigma}_{23} &= \bar{\sigma}_{32} = \bar{p}_2 \\
 \bar{\sigma}_{33} &= \bar{p}_3
 \end{aligned}
 \tag{4}$$

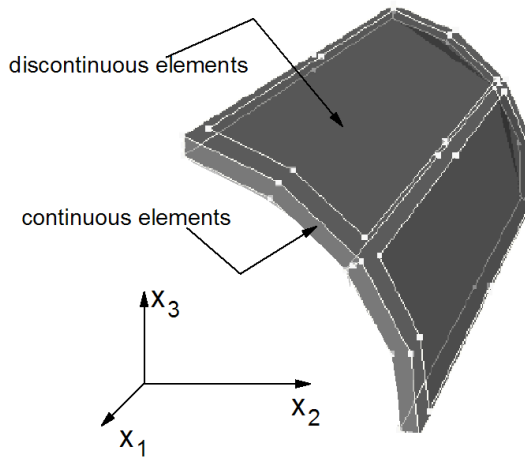


Figure 1: Thin-walled domain discretized with boundary elements

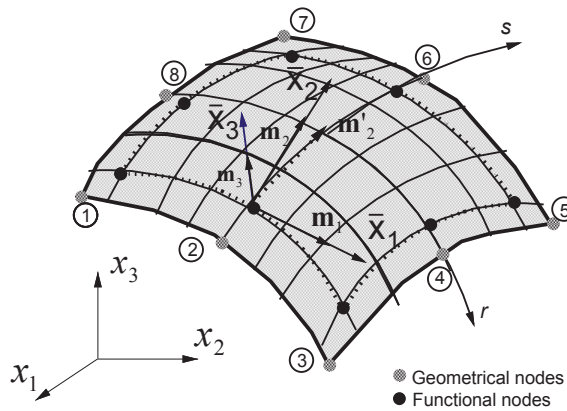


Figure 2: Local (node-based) reference system

Thus, only three more stress components have to be calculated, namely, those related to the tangential  $\bar{x}_2$ - $\bar{x}_3$  plane,  $\bar{\sigma}_{11}$ ,  $\bar{\sigma}_{22}$ , and  $\bar{\sigma}_{12}$ , which are given by

$$\begin{aligned} \bar{\sigma}_{11} &= \frac{1}{(1-\nu)} [\nu \bar{p}_3 + 2G(\bar{\epsilon}_{11} + \nu \bar{\epsilon}_{22})] \\ \bar{\sigma}_{22} &= \frac{1}{(1-\nu)} [\nu \bar{p}_3 + 2G(\bar{\epsilon}_{22} + \nu \bar{\epsilon}_{11})], \\ \bar{\sigma}_{12} &= 2G\bar{\epsilon}_{12} \end{aligned} \tag{5}$$

wherein the local strain components  $\bar{\epsilon}_{ij}$ ,  $i, j = 1, 2$ , in (5) are calculated by

$$\bar{\epsilon}_{ij} = \frac{1}{2} \left( \frac{\partial \bar{u}_i(x_1, x_2, x_3)}{\partial \bar{x}_j} + \frac{\partial \bar{u}_j(x_1, x_2, x_3)}{\partial \bar{x}_i} \right), \tag{6}$$

wherein

$$\frac{\partial \bar{u}_i(\mathbf{x})}{\partial \bar{x}_1} = \frac{\lambda_{ik}}{J(r)} \frac{\partial u_k(\mathbf{x})}{\partial r} = \frac{\lambda_{ik}}{J(r)} \left( \sum_{q=1}^{nnoel} \frac{\partial h_q(r, s)}{\partial r} u_{kq} \right), \tag{7}$$

$$\frac{\partial \bar{u}_i}{\partial \bar{x}_2} = \frac{1}{\bar{m}'_{22}} \left( \frac{\partial \bar{u}_i}{\partial \bar{x}'_2} - \frac{\partial \bar{u}_i}{\partial \bar{x}_1} \bar{m}'_{12} \right), \tag{8}$$

with

$$\frac{\partial \bar{u}_i(\mathbf{x})}{\partial \bar{x}'_2} = \frac{\lambda_{ik}}{J(s)} \frac{\partial u_k(\mathbf{x})}{\partial s} = \frac{\lambda_{ik}}{J(s)} \left( \sum_{q=1}^{nnoel} \frac{\partial h_q(r, s)}{\partial s} u_{kq} \right). \tag{9}$$

Above,  $h_q(r, s)$  denotes the isoparametric shape function associated with the  $q$ -th element node,  $J(s)$  is the Jacobian corresponding to its geometrical mapping into the natural coordinates, and  $nnoel$  is the number of nodes per element. The expression (8) is needed for  $\bar{x}'_2$  is not necessarily perpendicular to  $\bar{x}_1$ . The  $\bar{\mathbf{m}}'_2$  vector is the unit tangent vector given by  $\bar{\mathbf{m}}'_2 = \mathbf{dl}_2 / \|\mathbf{dl}_2\|$ , where  $\mathbf{dl}_2 = \mathbf{dx} / \|\mathbf{ds}\|$  is expressed in relation to the local system. All the boundary stresses are calculated at the geometrical contour of the boundary elements, which are always continuous. In case of discontinuous elements, the displacement fields at the geometrical contour of the boundary elements are first determined via the interpolation functions for the discontinuous elements, before the stress calculation procedure described above be applied. The global stress tensor is obtained by rotating the local stress tensor,  $\bar{\sigma}$ , to the global coordinate system via  $\sigma = \mathbf{R}\bar{\sigma}\mathbf{R}^T$ . By taking then, say, the global stress tensor,  $\sigma$ , at any boundary point, the corresponding principal stresses can be easily obtained by solving the eigenvalue problem  $\sigma \mathbf{x}_i = \sigma_i \mathbf{x}_i$ , wherein  $\sigma_i$  and  $\mathbf{x}_i$ ,  $i=1,2,3$  are the principal stresses and corresponding principal directions

#### 4 Applications

To show how the strategy for stress calculation on boundary nodes performs, a thin-walled steel beam under shear load, a thick rectangular-cross-section beam, and a carbon-nanotube-reinforced composite (CNT composite) under axial deformation are analyzed. In the graph legends, the results calculated with the formulation presented in this paper are identified by NAESY acronym, which stands for the computational code name into which the formulation has been incorporated. In general, the NAESY results have been compared to the corresponding ANSYS-13 ones. In all BE analyses (with the NAESY code), the quadratic 8-node (continuous or discontinuous) boundary element is employed, and in all FE analyses (with the ANSYS-13 code), the 20-node SOLID-186 brick finite element is used.

##### 4.1 Thin-walled steel beam under uniform load

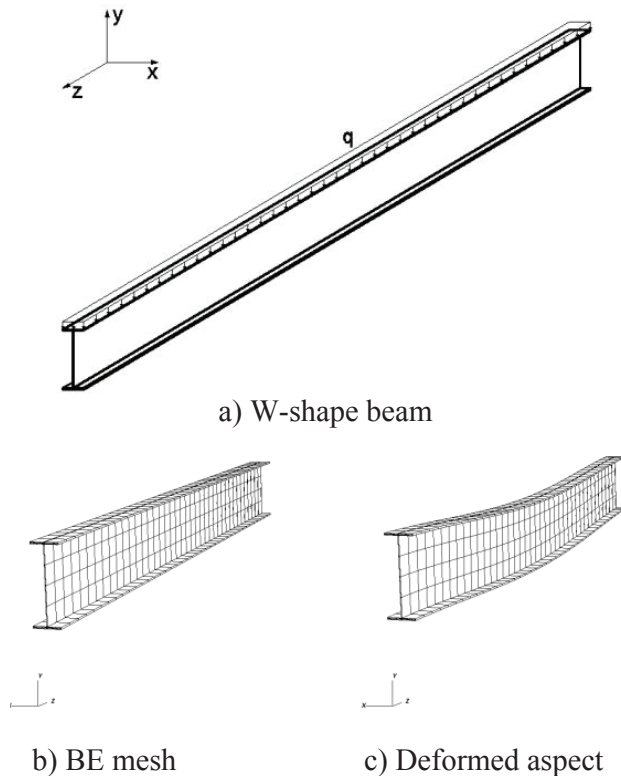


Figure 3: Thin-walled steel beam under load  $q$

In this example, the thin-walled steel beam shown in Fig. 3, 4m long, clamped at both ends and subjected to a uniformly distributed load  $q=15kN/m^2$  (Fig. 3a), is analyzed. Its W- shape cross section has the following measures:  $b_f=140mm$  (flange width),  $t_f=9.5mm$  (flange thickness),  $h_w=381mm$  (web height), and  $t_w=4.75mm$  (web thickness). The steel parameters considered are  $E=200GPa$  (elasticity modulus), and  $\nu=0.3$  (Poisson’s ratio). Three subregions are employed to model this beam (two subregions for the flanges and one for the web), and the corresponding BE mesh (see Fig. 3b) has a total of 1092 boundary elements (4704 nodes and 14.112 degrees of freedom). In Fig. 3c, the global deformed aspect of the beam is presented, and to more precisely verify the correctness of the NAESY results, the same problem has been analyzed with the ANSYS-13 software employing a mesh with 5394 SOLID-186 finite elements (38,786 nodes, 116,358 degrees of freedom), and the  $\sigma_{zz}$  normal stress component and von Mises stresses along the beam axis obtained with both codes have been contrasted.

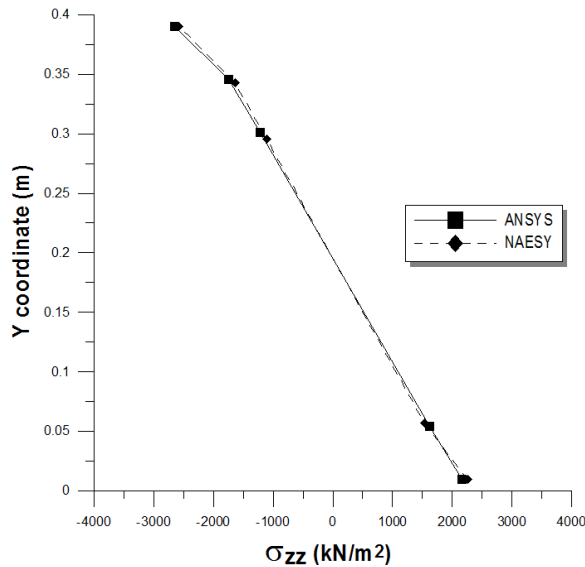


Figure 4:  $\sigma_{zz}$  along the central cross-section

Particularly for the middle-span cross-section of the beam, the results are shown in Fig. 4 ( $\sigma_{22}$  normal stress component), and in Fig. 5 (von Mises stresses,  $\sigma_v$ ).

#### 4.2 Cantilever beam under uniform load

In this problem, the cantilever beam shown if Fig. 6, with length  $l = 3m$ , under a uniformly distributed load  $q=15kN/m^2$ , is analyzed. The geometric details of the

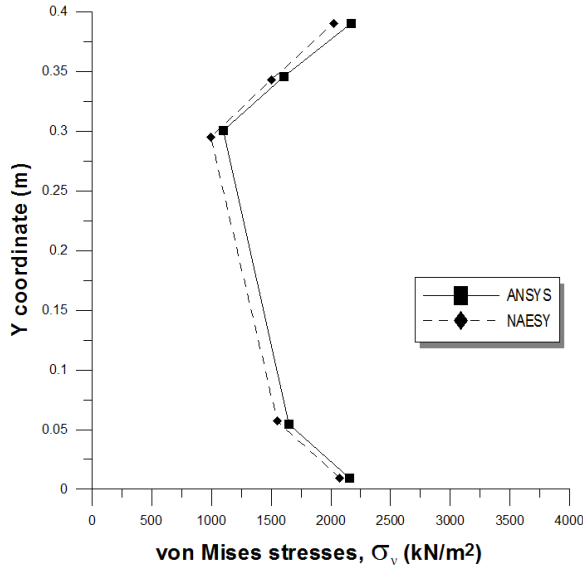


Figure 5: von Mises stresses,  $\sigma_v$ , at the central cross section

beam cross-section are:  $b = 0.2m$ , and  $h = 0.3m$  The BE mesh and corresponding deformed aspect are given in Fig. 7a and Fig. 7b respectively.

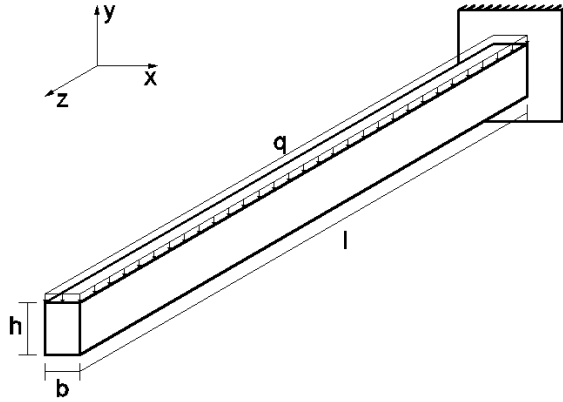
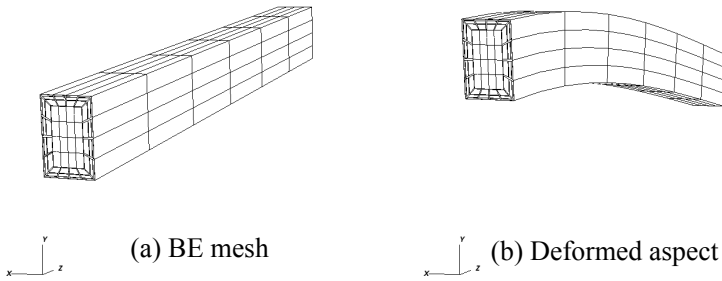


Figure 6: Cantilever beam under uniform load  $q$

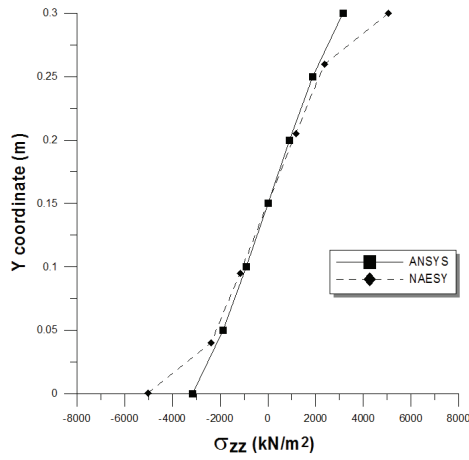
The material parameters adopted for the beam are  $E=21.7GPa$  (elasticity modulus), and  $\nu=0.2$  (Poisson’s ratio). The BE beam model (NAESY model) considered consists of only one subregion with 176 8-node boundary elements (corresponding to

Figure 7: Cantilever beam under load  $q$ 

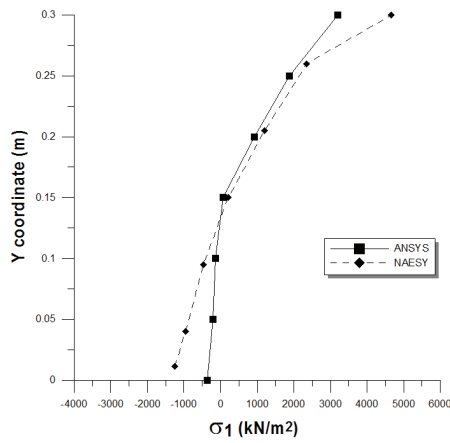
802 nodes and 2406 degrees of freedom). On the other hand, 360 20-node finite elements (SOLID 186) are employed to construct the ANSYS model (with 2013 nodes and 6039 degrees of freedom). To show the accuracy of the BE responses, the  $\sigma_{zz}$  stress component, and the largest and smallest principal stress components,  $\sigma_1$  and  $\sigma_3$ , are plotted at the clamped end of the cantilever (Fig. 8). As observed from the stress curves in Fig. 8, the BE (NAESY) and FE (ANSYS) stress values close to the superior and inferior beam surfaces considerably differ from each other, with the BE stress values much higher than the corresponding FE ones. In fact, the stresses values in these points theoretically go to infinity, and these results just confirm the ability the BEM has to appropriately describe this behavior.

### 4.3 CNT-based composite

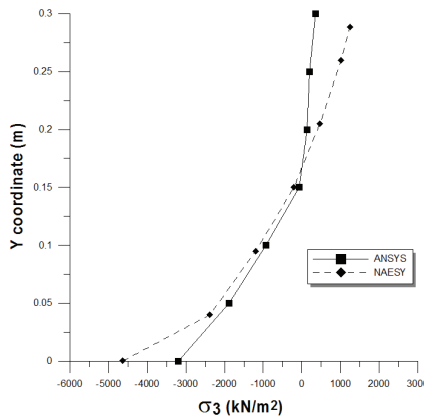
In this application, the CNT-fiber reinforced composite shown in Fig. 9 under  $\bar{\delta}_z = -1.0$  (shortening in  $z$  direction) is analyzed. The long CNT fibers are geometrically defined by cylindrical tubes having outer radius  $r_0 = 5.0 \text{ nm}$  and inner radius  $r_i = 4.6 \text{ nm}$ , and length  $l_f = 10 \text{ nm}$ . Its material properties are  $E_{CNT} = 1,000 \text{ nN} \cdot \text{nm}^{-2} (\text{GPa})$ , and  $\nu_{CNT} = 0.3$ , and for the host material (polymeric matrix),  $E_m = 100 \text{ nN} \cdot \text{nm}^{-2} (\text{GPa})$ , and  $\nu_m = 0.3$ . The BE model employed consists of 8 subregions with 7980 degrees of freedom (Fig. 9a). This problem has been considered in Araujo and Gray (2008) to characterize CNT composites with various fiber-packing patterns. In Araujo, d'Azevedo and Gray (2011) all the details of the loadings considered for determining the equivalent material properties are given. Here, just a sample of response, namely the  $\sigma_{zz}$  component, is shown (Fig. 9b). Here, the block-diagonal SBS-based preconditioned BiCG with tolerance number  $\zeta = 10^{-8}$  is applied. The boundary stress values calculated are compatible with those obtained in previous papers (Araujo and Gray 2008; Araujo, d'Azevedo and Gray 2011; Chen and Liu 2004). In this model, discontinuous boundary elements with  $d = 0.10$  are employed when needed.



(a)  $\sigma_{zz}$  as a function of the height

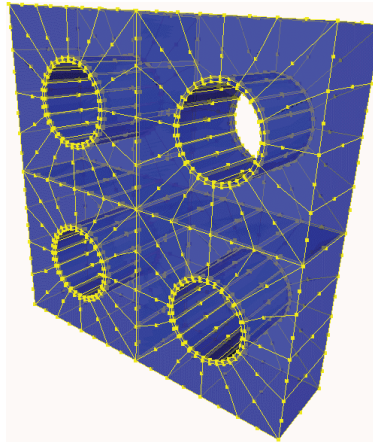


(b)  $\sigma_1$  (largest principal stress) as a function of the height



(c)  $\sigma_3$  (smallest principal stress) as a function of the height

Figure 8: Stress components at the clamped end of the beam



(a) BE mesh (8 subregions, 7980 degrees of freedom)

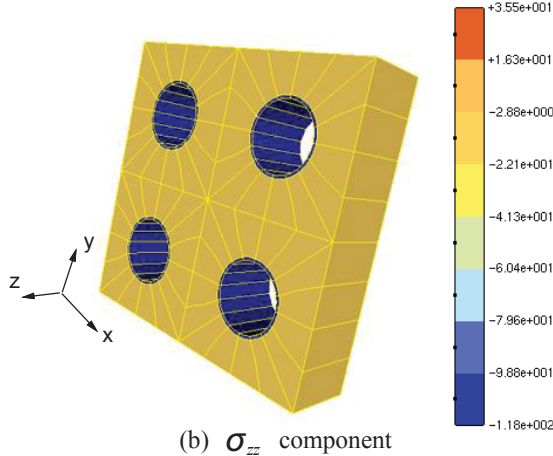
(b)  $\sigma_{zz}$  component

Figure 9: CNT-based composite

## 5 Conclusions

In this paper, the BE SBS technique proposed in previous papers [Araujo and Gray 2008; Araujo, d'Azevedo and Gray (2011)] is incremented with routines for the calculation of stresses at the boundary nodes. As shown at the light of the intricate problems analyzed in this paper, the stress-calculation technique employed, based on the direct application of Hooke's law, allows accurately and efficiently calculating strain and stress at boundary element nodes without evaluating the strongly singular and hypersingular boundary integrals involved in standard BEM formulations. This is very important for determining the stress-tensor fields in thin-walled

domains, wherein in fact only the boundary stress fields are needed. Along with the whole boundary- element SBS technique, including its straightforward parallel-computing implementation, the strategy proposed in this paper may be fundamental for analyzing general composites, and for the microstructural analysis of materials.

**Acknowledgement:** This research was sponsored by the Brazilian Research Council (CNPq), and by the Research Foundation for the State of Minas Gerais (FAPEMIG).

## References

- Araújo, F. C.** (1994): *Time-Domain Solution of Three-dimensional Linear Problems of Elastodynamics by means of a BE/FE Coupling Process (in German)*, Ph.D. Thesis. T.U. Braunschweig, Germany.
- Araújo, F. C.; Gray, L. J.** (2008): Evaluation of effective material parameters of CNT reinforced composites via 3D BEM. *Comp. Mod. Eng. Sci.*, vol. 24, no. 2, pp. 103-121.
- Araújo, F. C.; d’Azevedo, E. F.; Gray, L. J.** (2010): Boundary-element parallel-computing algorithm for the microstructural analysis of general composites. *Computers & Structures*, vol. 88, pp. 773-784.
- Araújo, F. C.; d’Azevedo, E. F.; Gray, L. J.** (2011): Constructing efficient substructure-based preconditioners for BEM systems of equations. *Eng. Anal. Boundary Elements*, vol. 35, pp. 517–526.
- Barrett, R.; Berry, M.; Dongarra, J.; Eijkhout, V.; Romine, C.** (1996): Algorithmic bombardment for the iterative solution of linear systems: A poly-iterative approach. *J. Comp. Appl. Mathematics*, vol. 74, pp. 91-109.
- Benedetti, I.; Aliabadi, M. H.** (2013): A three-dimensional cohesive-frictional grain-boundary micromechanical model for intergranular degradation and failure in polycrystalline materials. *Computational Materials Science*, vol. 67, pp. 249-260.
- Brebbia, C. A.; Telles, J. C. F.; Wrobel, L. C.** (1984): *Boundary Element Techniques: Theory and Applications in Engineering*. Springer-Verlag, Berlin.
- Chen, X. L.; Liu, Y. J.** (2004): Square representative volume elements for evaluating the effective material properties of carbon nanotube-based composites. *Comput. Mat. Sci.* **29**, pp. 1-11.
- Chen, K.** (2005): *Matrix Preconditioning Techniques and Applications*. Cambridge, UK, Cambridge University Press.
- Dong, L.; Atluri, S. N.** (2012): Development of 3D Trefftz Voronoi cell finite elements with ellipsoidal voids and/or elastic/rigid inclusions for micromechanical

modeling of heterogeneous materials. *CMC: Computers Materials and Continua*, vol. 29, no. 2, pp. 39-81.

**Dong, L.; Atluri, S. N.** (2013): SGBEM Voronoi cells (SVCs) with embedded arbitrary-shaped inclusions, voids, and/or cracks, for micromechanical modeling of heterogeneous materials. *Computers, Materials and Continua*, vol. 33, no. 2, pp. 111-154.

**Ghoniem, N. M.; Cho, K.** (2002): The emerging role of multiscale modeling in nano- and micro-mechanics of materials. *Computer Mod. Eng. Sci.*, vol. 3, pp. 147-174.

**Hughes, T. J. R.; Levit, I.; Winget, L.** (1983): An element-by-element solution algorithm for problems of structural and solid mechanics. *Comput. Methods Appl. Mech. Engrg.*, vol. 36, no. 2, pp. 241-254.

**Kitipornchai, S.; He, X. Q.; Liew, K. M.** (2005): Buckling analysis of triple-walled carbon nanotubes embedded in an elastic matrix. *J. Appl. Phys.*, vol. 97, pp. 114318

**Namilae, S. ; Chandra, U.; Srinivasan, A; Chandra, N.** (2007): Effect of interface modification on the mechanical behavior of carbon nanotube reinforced composites using parallel molecular dynamics simulations. *CMES: Computer Modeling in Engineering and Sciences*, vol. 22, no. 3, pp. 189-202.

**Pantano, A; Parks D. M.; Boyce, M. C.** (2004): Mechanics of deformation of single and multiwall carbon nanotubes. *J. Mech. Phys. Solids*, vol 52, pp. 789-821.

**Sleijpen, G. L. G.; Fokkema, D. R.** (1993): BICGSTAB(L) for linear equations involving unsymmetric matrices with complex spectrum. *Electronic Trans. Num. Methods Anal.*, vol. 1, pp. 11-32.

**Srivastava1, D.; Atluri, S. N.** (2002): Computational nanotechnology: a current perspective. *CMES: Computer Mod. Eng. Sci.*, vol. 3, pp. 531-538.

**Van der Vorst, H. A.** (2003): *Iterative Krylov Methods for Large Linear Systems*. Cambridge University Press.

**Wang, C. M; Ma, Y. Q.; Zhang, Y. Y; Ang, K. K.** (2006): Buckling of double-walled carbon nanotubes modeled by solid shell elements. *Journal of Applied Physics*, vol. 99, pp. 114317.

**Zhang, S.-L.** (2002): A class of product-type Krylov-subspace methods for solving nonsymmetric linear systems. *Comp. and Appl. Math.* vol. 149, pp. 297–305.